Lawrence Berkeley National Laboratory
Recent Work

Title

New Developments in Soft X-ray Monochromators for 3rd Generation Synchrotron Radiation Sources

Permalink

https://escholarship.org/uc/item/4m78z0j6

Journal

Journal of Electron Spectroscopy, 75(Dec)

Authors

Padmore, H.A.
Warwick, T.

Publication Date

1995-06-08

eScholarship.org Powered by the California Digital Library
University of California

LBL-37381
UC-410
Preprint

Lawrence Berkeley Laboratory
UNIVERSITY OF CALIFORNIA

Accelerator & Fusion Research Division

Submitted to Journal of Electron Spectroscopy

New Developments in Soft X-Ray Monochromators for 3rd Generation Synchrotron Radiation Sources

H.A. Padmore and T. Warwick

June 1995

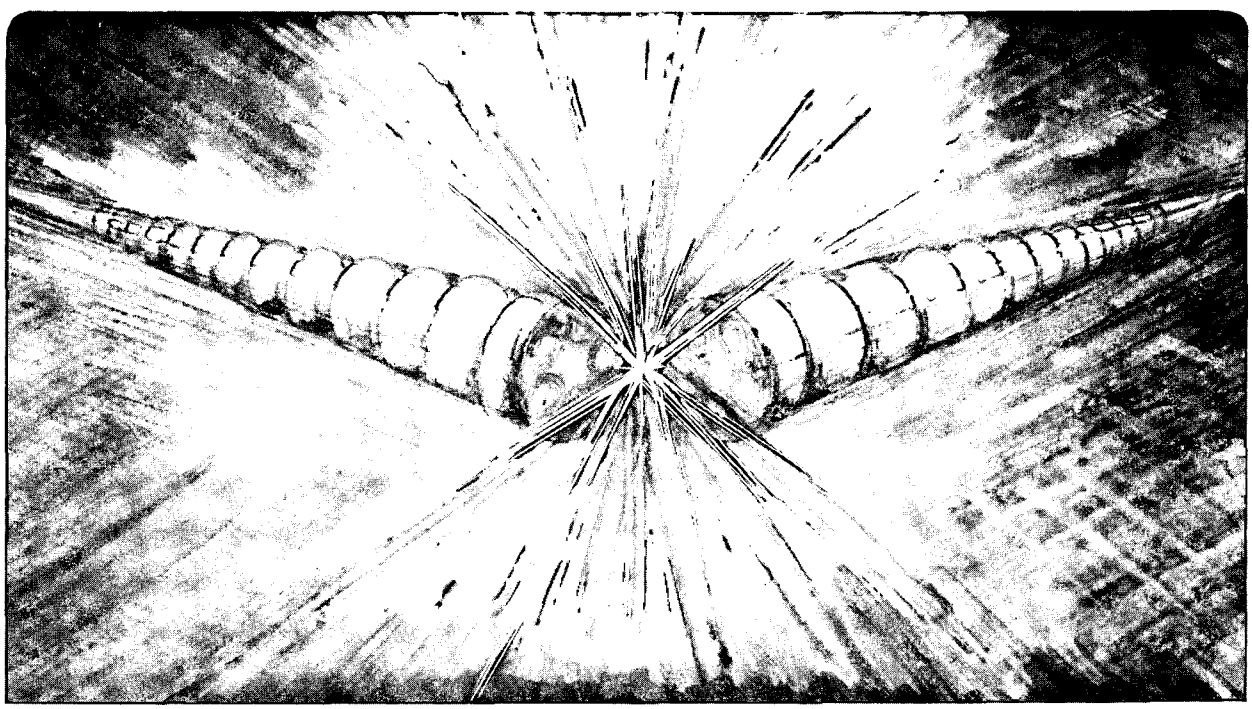

REFERENCE COPY
Does Not
Circulate
Copy 1
LBL-37381
Bldg. 50 Library.

Prepared for the U.S. Department of Energy under Contract Number DE-AC03-76SF00098

DISCLAIMER

This document was prepared as an account of work sponsored by the United States Government. While this document is believed to contain correct information, neither the United States Government nor any agency thereof, nor The Regents of the University of California, nor any of their employees, makes any warranty, express or implied, or assumes any legal responsibility for the accuracy, completeness, or usefulness of any information, apparatus, product, or process disclosed, or represents that its use would not infringe privately owned rights. Reference herein to any specific commercial product, process, or service by its trade name, trademark, manufacturer, or otherwise, does not necessarily constitute or imply its endorsement, recommendation, or favoring by the United States Government or any agency thereof, or The Regents of the University of California. The views and opinions of authors expressed herein do not necessarily state or reflect those of the United States Government or any agency thereof, or The Regents of the University of California.

Lawrence Berkeley National Laboratory
is an equal opportunity employer.

DISCLAIMER

This document was prepared as an account of work sponsored by the United States Government. While this document is believed to contain correct information, neither the United States Government nor any agency thereof, nor the Regents of the University of California, nor any of their employees, makes any warranty, express or implied, or assumes any legal responsibility for the accuracy, completeness, or usefulness of any information, apparatus, product, or process disclosed, or represents that its use would not infringe privately owned rights. Reference herein to any specific commercial product, process, or service by its trade name, trademark, manufacturer, or otherwise, does not necessarily constitute or imply its endorsement, recommendation, or favoring by the United States Government or any agency thereof, or the Regents of the University of California. The views and opinions of authors expressed herein do not necessarily state or reflect those of the United States Government or any agency thereof or the Regents of the University of California.

LBL-37381
UC-410

NEW DEVELOPMENTS IN SOFT X-RAY MONOCHROMATORS FOR 3RD GENERATION SYNCHROTRON RADIATION SOURCES*

H.A. Padmore and T. Warwick

Advanced Light Source
Accelerator and Fusion Research Division
Lawrence Berkeley Laboratory
University of California
Berkeley, CA 94720, USA

Invited paper to be published by the Journal of Electron Spectroscopy

*This work was supported by the Director, Office of Energy Research, Office of Basic Energy Sciences, Materials Sciences Division, of the U.S. Department of Energy, under Contract No. DE-AC03-76SF00098.

New Developments in Soft X-ray Monochromators for 3rd Generation Synchrotron Radiation Sources

H. A. Padmore and T. Warwick

Advanced Light Source, Accelerator and Fusion Research Division,
Lawrence Berkeley Laboratory, Berkeley, CA 94720, USA

Abstract

The advent of 3rd generation synchrotron soft x-ray radiation sources has opened up many new opportunities for the use of spectroscopy and microscopy to study the structure of complex materials. The ultra-high brightness of these sources offers the possibility of combining these techniques so that the spectroscopy of microscopic areas of a material may be studied (spectromicroscopy), and in addition offers tremendous flux and resolution enhancements for traditional macroscopic surface studies. The optical properties of both bending magnet and undulator sources on third generation soft x-ray sources offers significant possibilities for improving the performance of optical systems over traditional designs. We will describe two recent such advances in beamline optical system design at the Advanced Light Source (ALS) and review the performance of a current generation of undulator based beamline at the ALS.

1. Introduction

The current generation of undulator based soft x-ray monochromators evolved through many stages from the systems used on the first synchrotron radiation sources. These early designs used bending magnet radiation, and in many cases were based on systems that had traditionally been applied to laboratory sources. These sources such as discharge lamps at low energy and bremstrahlung continuum sources at high energy emitted radiation isotropically and were in general weak, and so the designer's goal was to collect as large an aperture as possible whilst at the same time controlling aberrations. Soft x-rays from a bending magnet source are highly collimated in the vertical direction and are isotropically emitted in the horizontal direction. This difference in the source characteristics ultimately

drove the evolution of designs away from concepts adapted from laboratory instrumentation to ones that were uniquely suited to the special radiation characteristics of bending magnet sources. This process led to the two main designs seen at synchrotron radiation sources today, the SX700 style of plane grating monochromator [1] and the non-Rowland spherical grating monochromator (SGM) [2,3,4]. We will deal here only with the development of the SGM.

The SGM has been enormously successful in opening up the field of high resolution soft x-ray core level spectroscopy. It combines simplicity with the possibility of collecting a large non-dispersive aperture, is reliant on only one optical element for high resolution, uses a spherical diffracting surface that is relatively easy to fabricate with a low slope error, and decouples the resolution from the source point location in the non-dispersive direction. It does however require defocus to be eliminated by the use of a translating exit slit, and suffers from a finite amount of coma aberration, except at one energy where the Rowland circle condition is satisfied. This latter problem can be solved over limited energy ranges by translating both the entrance as well as the exit slit in order to satisfy the Rowland condition [3], but at the expense of flux passing through the slit. Another solution to this problem combines the variable included angle concept of the SX700 with the SGM. A plane mirror is inserted between the entrance slit and the grating such that the included angle can be adjusted (VASGM). The focusing condition can now be exactly solved with fixed entrance and exit slits, by adjusting the included angle as a function of photon energy [5]. For one particular grating energy range, this adjustment is usually a fraction of a degree. If the exit slit position is allowed to be a variable, it can be shown that the Rowland condition can be satisfied over a significant energy range. The addition of a variable included angle in the design is crucial also in achieving a high diffraction efficiency over a wide energy range. Although the deviation angle tuning range of a VASGM is very small for a particular grating to stay in focus, this rotation mechanism can be put to further use by selecting included angle ranges for each grating which are give optimum efficiency. For example, a monochromator designed for 20 - 100 eV might have an included angle of 150°, but for energies up to 1500 eV might have an included angle of 176°. The included angle in a fixed angle design is set by the highest photon energy; the lower photon energies can then only be reached by reduction of the line density. It has been shown for laminar gratings that for a particular line density there is an optimum groove width, groove depth and included angle as a function of photon energy [6]. Deviation from these conditions can impose a severe loss of performance. The choice therefore has to be a variable angle design for a wide photon energy range coverage, or a

fixed angle design optimized for only a narrow energy range. In section 4 we give examples of these two types of design concept.

The characteristics of bending magnet sources on second generation machines, as well as the availability of reflective optical elements with spherical surfaces of high figure accuracy drove the evolution of monochromator design towards the use of spherical optics, both in the SGM and in later versions of the SX700 [5,7,8]. In designing monochromators that are suited for third generation synchrotron radiation sources, using both bending magnets and undulators, we must fully understand the special nature of the source in deciding the next evolutionary track that designs must follow. An additional constraint is imposed by the nature of the experiment. Almost all systems designed so far were for experiments on large area samples. The only design constraint in terms of the quality of focusing onto the sample was set by the acceptance of an analyzer, and typically a focus of 1 mm^2 was adequate. Third generation sources offer us the possibility of performing zone plate scanning microscopy, full field imaging microscopy, and high energy resolution spectroscopy on macroscopic samples. Each of these impose different demands on the type of focusing needed and in section 4 we give examples of designs for all three categories. In the next section, we therefore examine the characteristics of a third generation source, using the ALS as an example.

2. Optical characteristics of a third generation soft x-ray source

The Advanced Light Source is typical of the 3rd generation soft x-ray sources, and we will use it to illustrate the special features of this class of machine as it affects optical design. The ALS is a triple bend achromat structure with twelve fold symmetry, and has a horizontal emittance of around 4×10^{-9} m.rads. The lattice function is shown in Fig. 1. The three bending magnets in one superperiod are marked by B1, B2 and B3, QF and QD are focusing and defocusing quadrupole magnets and SF and SD are the equivalent sextupoles. The superperiodicity is shown folded about the center of a straight section. The straight sections in the ALS can accommodate undulators up to 5 m in length. The figure shows the value of the horizontal and vertical beta functions and the dispersion as a function of position within the cell. The beam size and divergence around the storage ring are modulated by the beta function, and for the special conditions of a zero gradient (waist) are given by the following relations,

$$\sigma_y = \sqrt{\varepsilon_y \beta_y} \qquad \sigma_{y'} = \sqrt{\frac{\varepsilon_y}{\beta_y}} \tag{1}$$

$$\sigma_x = \sqrt{\varepsilon_x \beta_x + \left(D_x \frac{\delta\rho}{\rho}\right)^2} \qquad \sigma_{x'} = \sqrt{\frac{\varepsilon_x}{\beta_x} + \left(D'_x \frac{\delta\rho}{\rho}\right)^2}$$

where subscript x,y indicates the horizontal and vertical directions, σ is the rms source size, σ'is the rms divergence, ε is the emittance of the electron beam, β is the beta function, D is the dispersion and $\delta\rho/\rho$ is the momentum spread of the electron beam. In the absence of alignment and field errors, the vertical emittance is zero, but in practice a value of a few percent of the horizontal emittance is typical. In the case of the ALS, the vertical emittance is around 1×10^{-10} m.rads. From Fig. 1 and (1) it can be seen that the vertical beam size is maximum in the outer pair of dipole magnets, minimum in the center dipole, and about double the minimum value in the straight sections. The actual rms values of beam size for the outer dipoles, the center dipole and the center of the insertion device straight are 45, 9 and 20 μm respectively. In the horizontal direction, from (1) it can be seen that dispersion is an additional factor that must be added to the beam size. This effect is simply that as electrons of different energies pass through a bending magnet they are dispersed in position and angle. The storage ring has a natural energy spread related to the emittance, and in addition this can be increased by effects such as the coupled bunch instability whereby a following electron bunch picks up the higher modes of the resonant RF cavity excited by the passage of the preceding bunch. This effect can be eliminated by a longitudinal feedback system, or by mode damping the RF cavity. For the ALS, the natural energy spread is around 7×10^{-4} (RMS). The straights are designed to be dispersion free to decrease the effects of high strength undulators on the emittance, and so the energy spread does not translate into an increase in horizontal source size in these locations. The rms horizontal source size in the straights is 210 μm. In the outer and center dipoles, the rms horizontal source size is 44 μm and 85 μm respectively. The divergence of the electron beam is vanishingly small compared to the opening angle of the radiation from a dipole magnet. For example, the rms vertical divergence at the center dipole is 8 μrad compared to a typical photon beam divergence in the soft x-ray energy range of 500 μrad. For a spectroscopic experiment using a vertically dispersing monochromator, the center bending magnet is superior due to its smaller vertical source size; this translates into more flux at high resolution where the imaged source would overfill the entrance slit, or for an entrance slitless monochromator to higher resolution. For some types of application, such

as directly imaging the source with a condensor zone plate, the rounder beam provided by the outer dipole magnet sources would be superior.

An important point should be noted from the above description. The source area of the center dipole is about two orders of magnitude smaller than a typical dipole source at a second generation synchrotron facility. This opens up the possibility that these sources can be used for microscopy, especially for full field applications where the object is to illuminate a small area that is then imaged at high magnification with an x-ray or electron optical system. In section 4, we will give an example of such an application.

For the dipole sources discussed above, the source size is dependent on the electron beam size and the angular properties are those of a single electron passing through the dipole. This is because in the soft x-ray energy range, for a typical photon beam divergence of 0.5 mrads (rms) in the vertical direction, the corresponding diffraction limited source size is a few μm, smaller than the electron beam size. In addition, the electron beam divergence is much smaller than the typical divergence and can hence be neglected. For undulator sources the situation is more complex. The divergence and diffraction limited source size of the radiation pattern produced by a single electron passing through an undulator are given by,

$$\sigma_{r'} = \sqrt{\frac{\lambda_n}{L}} \qquad \sigma_r = \frac{1}{4\pi}\sqrt{\lambda L} \qquad (2)$$

where $\sigma_{r'}$ and σ_r are the rms divergence and diffraction limited source size respectively, L is the length of the undulator and λ is the wavelength radiated. For example, a 4.5 m long undulator as at the ALS, radiating at the carbon K edge (44Å), will produce an rms divergence and source size of 31 μrads and 11 μm respectively. This is to be compared to the horizontal and vertical electron beam divergences and sources sizes of [210 μm, 19 μrad]$_h$ and [20 μm, 5 μrad]$_v$. It can be seen that the source size is dominated by the electron beam, but the divergence is dominated by the single electron photon beam divergence. It can also be seen that the source area is significantly bigger than that in a center bending magnet source.

The advantages of an undulator source over a bending magnet source are primarily twofold, firstly the very small divergence of the light, and secondly the high flux contained within that small angle. The flux radiated within this central cone is given by,

$$F_n = 1.43 \times 10^{14} N Q_n I \qquad (3)$$

where N is the number of periods, I is the current (Amps), and Q_n is a parameter that depends on the deflection parameter K, and the harmonic number. For the first harmonic at a K of 1, $Q_n(K)$ is 0.55, and approaches 1 for values of K above 2.5. For the 5 cm period undulator (U5) at the ALS with 89 periods, and at the operating current of 400 mA, this therefore gives 3×10^{15} ph/sec in a bandwidth of 1/1000. This is the equivalent of the flux collected in a horizontal aperture of several hundred mrads of bending magnet radiation. For the example above of a 4.5m undulator at the carbon K edge, the divergence is a factor of 10 lower than that from a dipole source in the vertical direction at the same wavelength. The lower the divergence the higher can be the demagnification an optical system limited either by aberrations, or by the fundamental limit set by the ratio of the grazing angle of the central ray on a mirror to the convergence angle of the light from the mirror. However, for some cases such as full field microscopy at moderate spatial resolution, a high demagnification is unnecessary and so in these cases, bending magnet sources become more competitive with undulators. For other cases such as zone plate microscopy, only the central spatially coherent fraction of the beam can be used, and so central brightness becomes of prime importance and so an undulator is the source of choice. This interplay between the type of experiment, the source characteristics and the optimum optical system will be explored further in the two examples given in section 4.

3. Design and performance of undulator monochromators at the ALS

The undulator monochromators at the ALS are designed to take advantage of the special characteristics of the source whilst dealing effectively with the very high power load on the optical elements. As an example, Fig. 2 shows the layout of beamline 7.0, a system designed for the energy range 60 - 1200 eV and which uses an 89 period 5 cm period length undulator [9]. The performance of this system has been reported by Warwick et al [10] and a review of the design and performance has been given by Padmore and Warwick [11] in the context of the development of high performance undulator beamlines. We will briefly review the main points of the design here so that the development to the next generation of beamlines can be seen clearly.

Light from the 5 cm period undulator (U5) is first apertured in the horizontal direction by a pair of integrally cooled horizontal beam defining apertures. These are at a grazing angle of 7° to reduce the power density. This reduces the total power falling on the grating, as it is only the central quasi-coherent fraction of the beam that is required as given in equ. (2), not the full horizontal angular fan width. The latter is given by $\pm K/\gamma$ where K is the

deflection parameter and γ is the electron rest mass energy. For the U5, the minimum magnetic gap of the undulator is 14 mm, giving a K of 3.82, and corresponding to a total power of 1723 W, an angular horizontal power density of 853 W $mrad^{-1}$ and a central power density of 1602 W $mrad^{-2}$. The deflection angle is ± 1.3 mrads, in comparison to the rms divergence of the central cone of radiation of only 73 μrad, and so by setting a horizontal aperture to around 4σ, the total power falling onto the following optical element can be reduced by an order of magnitude. The effect of increasing the aperture size beyond that dictated to collect just the central cone is mainly to broaden the energy width of the undulator harmonic on the low energy side, and this also helps with reducing intensity noise induced by small angular oscillations of the beam.

The next element in the beamline is a vertically deflecting, integrally cooled spherical mirror, that focuses the source onto the entrance slit in the vertical direction. Integral cooling is necessary to preserve the < 1 μrad slope error tolerance of the optical surface dictated by the small vertical source size and the large source to mirror distance. The demagnification of this element onto the entrance slit of the monochromator is 15, and beam widths of around 7 μm have been experimentally measured. The entrance slits are intensively cooled, and suffer extremely high thermal stresses due to the high power and demagnification. Design calculations and measurements both show however that the position and width of the slits is stable to < 1μm for long periods.

Following the slits, the light passes into a standard Spherical Grating Monochromator (SGM). Although the optical design is 'standard', the execution for a high power beamline leads to some complex engineering issues. Again, due to the high heat load, the gratings have to be integrally cooled, and as with the other cooled elements are made from a dispersion strengthened copper alloy, Glidcop. They are therefore much more massive than in conventional monochromators, and the mechanisms for lateral translation of the three gratings, and for rotation need to be very stiff and are consequently large. In addition, this beamline was designed to achieve a resolving power of 10^4 in routine full aperture operation, and so the precision of rotation and overall stability were key issues. In practice the beamline achieved a resolving power of 10^4 at the nitrogen K edge without additional optical alignment after installation and appears to be highly stable. The exit slits are designed to track the monochromatic image position under computer control, and are mounted on a translation table attached to a massively stable granite block. After the slits the beam is deflected downward by a plane mirror, and then onto a cylindrical mirror with a variable tangential radius. This mirror is based on the design of Howells and Lunt [12] in which the thickness of the beam varies as the cube root of the distance from each end. Applying a point load to the center bends the mirror into a cylinder, and is applied in this

case with a programmable piezo actuator. The mirror therefore has a programmable radius, and this is necessary to focus the light from the longitudinally translatable exit slit to a fixed sample position. Light which has diverged in the horizontal direction through the monochromator is then focused by a cylindrical mirror at a demagnification of 14:1. An image size at the sample of less than 50 μm in diameter is routinely achieved. One important feature of the beamline is that two of these horizontal refocus mirrors are used to switch the beam into two independent end stations. One is used for microscopy, and one for spectroscopy. As both types of experiments have significant down time for sample mounting and surface preparation, this doubles the effective utilization of undulator beam. For energies less than 850 eV the monochromatic flux in a bandpass of 10^{-4} is > 10^{12} and for energies less than 200 eV is > 10^{13} photons/sec at 400 mA stored current for an electron beam energy of 1.5 GeV

Beamline 7.0 works to specification and has been in routine use for over one year. Due to thorough engineering, the downtime due to component failure in the beamline or due to realignment is negligible, and the beam is utilized effectively by using two horizontal refocus mirrors to deflect light into one of two end station branches. However, the beamline was designed to satisfy the needs of high resolution spectroscopy, and zone plate and full field microscopy. To a large extent, these requirements are incompatible. For example, high resolution spectroscopy requires a resolving power of near 10^4, where for most microscopy, a resolving power of 1000 is adequate. High spatial resolution full field photoelectron microscopy requires a variable illuminated area, from a few μm to a 100 μm, whereas often in spectroscopy, a large area is required to reduce radiation damage when illuminating over a long time. An example of the latter might be photoelectron diffraction, where although a single photoelectron spectrum takes only 10's of seconds, hundreds of spectra might be taken over a range of emission angles. A second and predictable problem is that a facility such as beamline 7.0 very rapidly gets overbooked, even after steps have been taken to increase the overall efficiency by using separate end stations with rapid beam switching, and with the use of fast sample entry systems.

In the next section we present designs that confront these two issues, and suggest a productive future direction for beamline designers.

4. Magnetic materials beamlines 7.3 and 4.0

We are currently building two new beamlines for the study of magnetic materials, bending magnet beamline 7.3 and undulator beamline 4.0. 7.3 addresses the issue of making high performance but inexpensive beamlines for a limited range of applications, but ones in which there will be extensive single purpose use. This beamline is designed for full field photoemission microscopy over the energy range 600 - 1300 eV, will satisfy most needs for magnetic imaging of surfaces at 100 nm spatial resolution, and will greatly reduce the pressure on undulator based beamlines. Undulator beamline 4.0 addresses the need for the ultimate in performance and offers the possibility for both high flux high resolution spectroscopy over a large energy range, as well as optimized systems for zone plate and full field microscopy.

4.1 Bending magnet beamline 7.3

The objective in designing beamline 7.3 was to arrive at a system which was simple and inexpensive, but yet which offered high performance. The microscope that will be used will be a simple two stage electrostatic system, using a three element immersion lens objective and three element unipotential projector lens [14,15]. This type of microscope is capable of a resolution of around 100 nm for an accelerating potential of 10 KV , limited by chromatic aberration, when used with secondary electrons generated by the interaction of soft x-rays with solids. The maximum field size is around 100 μm, and for work at the spatial resolution limit, a minimum field of around 20μm is desirable. The energy range of the monochromator has to cover the magnetically important transition metal $L_{2,3}$ edges, and the rare earth $M_{4,5}$ edges, a range from about 600 to 1300 eV. The resolution of the beamline is determined by the type of imaging to be performed. In this case, contrast can be generated by recording the difference between images taken with left and right circularly polarized radiation. The dichroism between left and right circular polarization has a maximum in the region of the transition metal $L_{2,3}$ or rare earth $M_{4,5}$ white lines, and has a typical full width of around 1 eV. Clearly this is a moderate resolution experiment, and operating at a resolving power of 1000 is adequate.

The optical arrangement we have chosen to use is shown in Fig. 3. It uses a bending magnet source from the center magnet of the ALS triplet structure. As mentioned in section 2, the source size has rms values of 9μm vertical by 85 μm horizontal. This means that a 1:1 vertical magnification of the monochomator would give us a monochromatic image size of < 30 μm (fwhm), in accordance with our needs for high spatial resolution imaging. In the horizontal direction, the source is much larger, and we need to demagnify by at least 6.5 : 1 to get a beam size of < 30 μm. In order to get the highest throughput, we

use an entrance slitless design working in negative order. A normal SGM focuses at around 1:1 magnification if the two defocus zero points are symmetrically located in the operating energy range as is the situation here. The entrance slitless design achieves high throughput by reducing the number of components to a minimum, and by the use of a low line density grating. In this case the line density can be reduced to 250 l/mm whilst still achieving adequate resolution, due to the small vertical source size and the long entrance arm length (12 m). Reduction of line density has two benefits; firstly, the dispersion of the system is reduced and matched to the experiment, and secondly the diffraction efficiency is increased. In a normal SGM the dispersion is not a variable parameter; it follows directly from the selection of the line density and the entrance arm length of the monochromator, if normal focusing behavior is required. In this case we are fortunate that the source size is about that required for the monochromatic image size; reducing the line density to around 250 l/mm gives the correct dispersion and source size limited resolution. It is important to realize that we can dispense with exit slits as the field of view of the microscope sets the energy resolution. For fields larger than the nominal 30 μm, we will see a dispersion of photon energy vertically across the sample, and we will need to correct for this by taking images at a few energies across this dispersed range.

The small line density also means that we will have a high diffraction efficiency. The diffraction efficiency of a lamellar profile grating is a function of deviation angle, groove depth, groove width, line density and coating material [6]. Fig. 4 shows as an example the optimization diagram for 300 and 1500 l/mm gold coated gratings. The upper panel shows the maximum diffraction efficiency that can be obtained if the optimum deviation angle, groove depth and groove spacing are used, as shown in the lower panels. It can be seen that for the 300 l/mm case for Fe L_3 at 700 eV the optimum deviation angle is around 175.5°, and that the diffraction efficiency will be 25% given the optimum groove depth and spacing. The equivalent for the 1500 l/mm grating is 10% diffraction efficiency at an optimum deviation angle of 173°.

The horizontal demagnification is provided by a single horizontally deflecting and focusing mirror. This will operate at a grazing angle of 2.5°, with a horizontal demagnification of 10:1, and accepts 2.5 mrads. This grazing angle of 44 mrads has to be compared to the convergence angle of the light from the mirror of 25 mrads; this ratio ultimately sets the maximum demagnification in the absence of aberrations. The coma-like aberrations of a spherical mirror would severely limit the image size, and so we will eliminate these by introducing a cubic correction into the surface figure. We will do this using the well known technique of unequal end couple bending, but using the monolithic

mirror bending technology pioneered by Howells and Lunt [12]. A quarter scale prototype mirror bender has achieved the required slope error tolerance of < 2.5 μradians (rms).

One penalty of using an entrance slitless design is that the photon energy will change if the vertical position of the source changes. In the case of the ALS, the beam is stable to around 4 μm (rms) over long periods if nothing is changed in the machine, but at present significantly larger changes are observed when undulators are scanned from open to closed, due to gap dependent dipole errors. These errors are compensated by a 'feed forward' algorithm which alters the strength of corrector magnets at the end of each undulator straight as a function of gap in a predetermined way. The strengths of the correction are measured using electron beam position monitors in the storage ring, and it is these that limit the ultimate accuracy of the method. Although this compensation system will be significantly improved in the near future by upgrading the beam monitor electronics, inevitably we will always suffer some vertical source motion at a level of a small fraction of the beam size. In this case our microscopy experiments will be relatively insensitive to small changes in photon energy as we will have an energy bandpass symmetrically located on one of the sharp 'white line' spectral features. However, we have designed a system that should be able to compensate for small motions of the source and keep a constant photon energy. This is shown in Fig. 3. The zero order beam from the grating will focus slightly nearer the grating than the first negative order, and will be deflected to a higher angle. We plan to place a split photodiode at this position, and feed the difference over the sum error signal back to the grating rotation drive. If the source moves from its nominal position, an error signal will be generated and the grating will rotate to produce a null signal on the photodiode. The angle between the zero order beam and the monochromatic beam absolutely encodes photon energy, and so it is only necessary to keep zero order stable on the split photodiode to stabilize energy.

The calculated photon flux in the monochromatic spot size of 30 μm (v) by 20 μm (h) is around 4×10^{12} at the nominal operating current of the storage ring, 400 mA. This photon flux density is 2 - 3 orders of magnitude higher than a typical beamline at a second generation source. This performance will be sufficient to achieve an acquisition rate of around 1 frame/sec at 100 nm resolution from many surface systems. This high performance is achieved by making the monochromator completely optimum for one purpose, full field photoelectron magnetic microscopy.

4.2 Undulator beamline 4.0

As we have seen in section 4.1, an optimally designed bending magnet beamline on a third generation source can offer extremely high performance for full field imaging. For other applications such as high resolution spectroscopy on dilute species, zone plate scanning microscopy and full field microscopy at higher spatial resolution, the performance of an undulator source is required. As previously discussed, the optical requirements of spectroscopy and microscopy are significantly different, and so for beamline 4.0, we have chosen to separate these areas into different beamlines.

Fig. 5 shows the approach we are taking. One of the most significant departures from normal design is that we are going to use two undulators in one straight section. These are 2.0 m in length, and three steering magnets, B1, B2 and B3 separate the beams from the two devices by 1.65 mrads. The generation of two beams from independent undulators has been used in the design of the Helios undulator at the European Synchrotron Radiation Facility [16,17]. However in this case we obtain the steering between the two devices by using separate electromagnets. The two undulators each have 4 rows of magnets, the 45° opposite pairs of which are capable of longitudinal translation [18, 19]. By adjusting the row phase, a pure vertical, horizontal or helical field can be produced, giving a horizontal linear polarization, vertical linear polarization or circular polarization. Fields of arbitrary helicity can be produced, and of opposite sign. One important feature is that whilst a helical trajectory produces only the first harmonic on-axis, an elliptical trajectory produces many harmonics, and this can be used to greatly extend the energy range of the device. The magnetic design of this Elliptically Polarizing Undulator (EPU) is reported in [20] and a description of the system can be found in [21].

Fig. 6 shows the brightness of the undulator for two periods, 7.5 cm and 5.0 cm at a machine operating energy of 1.9 GeV. The 5.0 cm undulator covers from 100 to 2000 eV using up to the fifth harmonic, and has optimum performance in the transition metal $L_{2,3}$ edge region. The 7.5 cm device covers down to 17 eV, and up to over 1000 eV. The need for two different periods is driven by the requirement to do valence band-mapping experiments at energies down to less than 20 eV, at the same time being able to probe deep core levels. It is not possible to design a single device to cover the entire energy range and so a system in which one has rapid interchange of undulators was selected. These two undulators occupy one of the two longitudinal positions in the undulator straight, and are interchanged by lateral translation. Two identical C type support structures are positioned on opposite lateral sides of the undulator straight, and interchange is accomplished with lateral translation of the floor plate the two structures are mounted on.

The second longitudinal position in the insertion device straight is occupied by a second 5.0 cm period undulator. The straight can therefore be occupied by a pair of 5 cm

devices or a 7.5 cm and a 5 cm period device. The reason for using a pair of 5 cm undulators is that we can set the photon energy to be the same from each, but we can set the helicities to be opposite by correct phasing of the jaws. By arranging for both beams to be recombined on the sample, we can switch helicity at high speed by mechanical chopping.

We are using two beamlines, one for high resolution spectroscopy (4.0.1), and one for microscopy (4.0.2). Using mirrors M1 and M2 (one set for each beamline) we can deflect both undulator beams into one beamline, or we can deflect one beam into each beamline. Selection of the appropriate mirror is done by lateral translation. The 4.0.1 monochromator will work with both the 7.5 and 5.0 cm period devices, and has a nominal operating range from 17 to 1800 eV. The beamline acceptance is set by the lowest photon energy and we have chosen to take an angular range of 4σ giving in this case 0.78 mrads. The large energy range requires the use of a monochromator with three different included angles, 150°, 170° and 176°. If a single included angle range was used, it would have to satisfy the upper photon energy limit, and would be non-optimum for low photon energies. In order to reach low photon energies, the line density would have to be reduced to impractically small values, and as shown from Fig. 4, would be highly non optimum. In practice a set of three plane mirrors at different angles will be located before the grating, and interchanged by lateral translation. With the addition of a small angular adjustment range about these primary values, we can correct for defocusing while maintaining a fixed exit slit position [5]. With the additional degree of freedom given by a variable included angle and a variable exit slit position, we can maintain the Rowland circle condition for a significant energy range. The horizontal focusing will be given by the M1/M2 horizontally deflecting spherical mirrors, and these will focus directly onto the sample. The vertical focusing onto the entrance slit of the monochromator will be produced by a vertically deflecting spherical mirror M3, and will demagnify the source by 6:1. Downstream of the grating, a rotating drum will be used to mechanically chop the beam between the individual right and left circularly polarized beams. Light diverging from the exit slit in the vertical direction will be refocused to the sample with a single cylindrical mirror. This overall arrangement has a high efficiency due to the use of optimum included angle ranges, has the capability for high spectral resolution, and has a very large photon energy range.

The 4.0.2 beamline for microscopy uses a similar M1/M2 mirror arrangement, except that the mirrors are plane. They are also designed with an angle such that the two horizontally divergent beams cross at the position of the grating. This should ensure that in changing between the two beams, the same area on the grating will be exposed, and

this should reduce energy shifts to a minimum. The monochromator itself is an entrance slitless SGM with one included angle of 175°, but with three gratings to cover the energy range from 100 to 1600 eV. The main operating range will be from 600 eV to 1600 eV for magnetic microscopy, but it was thought desirable to extend to lower than the carbon K edge, so that advantage could be taken of the ability of the undulators to produce horizontal and vertical linear polarization for linear dichroism studies. Downstream of the grating we will use a similar mechanical chopper to that used in the 4.0.1 beamline to switch between the beams in two beam mode. Two branchlines will be used after the grating, one for full field photoemission microscopy, and one for zone plate scanning microscopy. An M3-M6 4 mirror arrangement, similar to the M1/M2 system will be used to switch either both beams into one branchline, or one beam into each end station. The grating will focus on the apertures AP1 or AP2, and the horizontally deflecting and focusing spherical mirrors M3-M6 will focus at the same point at 6:1 horizontal demagnification. This full field microscope line has one extra stage of demagnification provided by a 20:1 demagnifying ellipsoidal mirror, which refocuses the divergent light from the exit aperture AP2 to the sample. This mirror will be located around 10 cm from the sample, inside the microscope experimental chamber. The expected beam diameter at the sample will be around 5 μm, but it will be increased up to 100 μm by moving the sample chamber longitudinally by 5 cm. For initial survey work at low magnification in the microscope, the illuminated field should be large (100μm), and for high resolution, the illuminated field should be much smaller (5μm). The most effective way to do this is to demagnify as much as possible onto the sample, and then to increase the beam size by moving the sample away from the focal plane. A full description of the beamline design can be found in [22].

It can be seen that the optical requirements for the two microscopy experiments and the spectroscopy experiment are significantly different. We have solved this problem by building two separate beamlines that are 'application specific'. In addition, extra flexibility is afforded by using three undulators in total, two 5 cm period devices that can be used independently or together with opposite helicities, and a 7.5 cm device for access to low photon energies. In addition, the use of two independent undulators in one straight section of the ALS doubles the possible number undulator based experiments.

5. Conclusions

We have attempted to show that the design of application specific optical systems offers significant advantages over traditional designs in which a multitude of different constraints have to be met. Clearly, bending magnet beamlines designed for flux density driven experiments such as full field microscopy can have very high performance when designed in this manner, and will significantly reduce the time pressure on undulator beamlines. The use of two simultaneously operating undulators in one straight offers flexibility, a doubling in capacity, and a method of fast switching between beams of opposite helicity.

Acknowledgments

The design, construction and commissioning of beamline 7.0 represents the work of many people, in particular Dick DiGennaro who led the engineering design team, Wayne McKinney who was responsible for the optical elements, Malcolm Howells who had the original concept for this type of system, and Phil Heimann who worked on the optical design. The work on diffraction grating theory is the result of a collaboration of several years with Vladimir Martynov, and the work on the elliptically polarizing undulator for beamline 4.0 is being carried out by Ross Schlueter and Steve Marks. The beamline design for 4.0 is a collaboration with Tony Young and on 7.3 with Tim Renner.

This work was supported by the Director, Office of Energy Research, Office of Basic Energy Sciences, Materials Sciences Division of the U.S. Department of Energy, under Contract no. DE-AC03-76SF00098.

References

1. H. Petersen, Opt. Commun. **40** (1982) 402

2. C. T. Chen, Nucl. Instrum. and Meth., **A256** (1987) 595

3. H. Hogrefe, M.R. Howells and E. Hoyer, SPIE **733** (1986) 274

4. H. A. Padmore, SPIE **733** (1986) 253

5. H. A. Padmore, Rev. Sci. Instr., **60** (1989) 1608

6. H. A. Padmore, V. Martynov and K. Hollis,
Nucl. Instrum. and Meth. **347** (1994) 206

7. R. Reininger and V. Saile, Nucl. Instrum. Meth. **A288** (1990) 343

8. H. Petersen, C. Jung, C. Hellwig, W. Peatman and W. Gudat, (1994),
Rev. Sci. Instrum., **66**(1995)1

9. A. Warwick and P. Heimann, Nucl. Instrum. Meth. **A319** (1992) 77

10. A. Warwick, P. Heimann, D. Mossessian, W. McKinney and
H. A. Padmore, Rev. Sci. Instr., **66**(2) (1995) 2037

11. H. A. Padmore and A. Warwick, J. Synchrotron Rad. **1** (1994) 27

12. M. R. Howells and D. Lunt, Optical Engineering **32**(8) (1993) 1981

13. G. Kaindl, K. Schultz, J. Bozek, F. Schlachter and P. Heimann,
Synch. Rad. News, **8**(4) (1995)

14. B. P. Tonner, G. R. Harp, S. F. Koranda and J. Zhang,
Rev. Sci. Instrum., **63** (1992) 564

15. B. P. Tonner and D. Dunham, Nucl. Instrum. Meth. **A 347** (1994) 436

16. P. Elleaume, Nucl. Instrum. Meth., **A291** (1990) 371

17. P. Elleaume and J. Chavanne, Nucl. Instrum. Meth., **A304** (1991) 719

18. S. Sasaki, K. Miyata and T. Takada, Jpm. J. Appl. Phys. **31** (1992) L1794

19. R. Carr and S. Lidia, SPIE **2013** (1993)

20. R. Schlueter and S. Marks, 14th Int. Conf. on Magnet. Technol., Finland, June 1995, submitted to IEEE Trans. on Magnetics

21. S. Marks, R. Schlueter, E. Hoyer, D. Plate and H. A. Padmore, to be submitted to Review of Scientific Instruments, Proc. of the Synchrotron Radiation Instrumentation Conf., Argonne, Oct. 1995

22. H. A. Padmore, A. Young, S. Marks and V. Martynov, to be submitted to Review of Scientific Instruments, Proc. of the Synchrotron Radiation Instrumentation Conf., Argonne, Oct. 1995

Figure Captions

Fig. 1

Diagram shows the beta and dispersion functions of the Advanced Light Source for one superperiod. B1, B2 and B3 are the three bending magnets of the triple bend achromat structure.

Fig. 2

Optical and geometrical layout of undulator beamline 7.0

Fig. 3

Schematic diagram showing the general arrangement of components in the magnetic microscopy bending magnet beamline 7.3

Fig. 4

Optimization diagrams are shown for gold coated lamellar gratings of line density 300 l/mm (left) and 1500 l/mm (right). The upper panel shows the maximum diffraction efficiency, the middle panel the required deviation angle, and the lower panel the required groove depths and widths. The 25, 50 and 75% lines in the middle panel show the deviation angles for these fractions of the maximum diffraction efficiency.

Fig. 5

The diagram shows the layout of undulator beamline 4.0. Two independent undulators are used, and light from either or both devices can be reflected into either of two beamlines. 4.0.1 is designed for high resolution spectroscopy, and 4.0.2 for microscopy.

Fig. 6

The merit function brightness of 7.5 cm (28 periods) and 5.0 cm period (40 periods) elliptically polarizing undulators for the ALS running at 1.9 GeV, 400 mA. The merit function brightness is defined as the product of the brightness and the square of the degree of circular polarization and is maximized in the region of the transition metal $L_{2,3}$ edges.

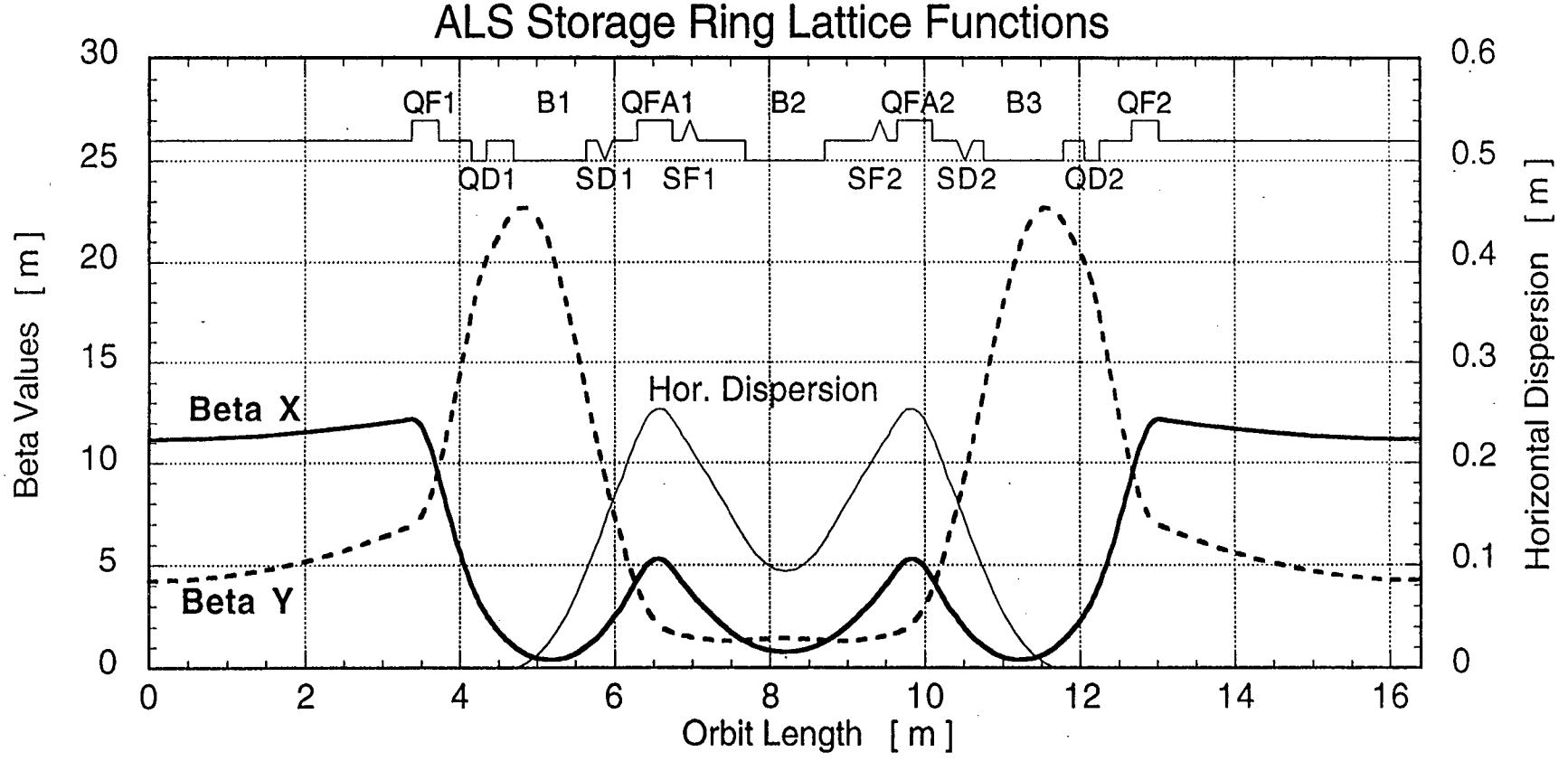
ALS Storage Ring Lattice Functions
QF1
B1
QFA1
B2
QFA2
B3
QF2
QD1
SD1
SF1
SF2
SD2
QD2
Beta X
Beta Y
Hor. Dispersion
Beta Values [m]
Horizontal Dispersion [m]
Orbit Length [m]
0
2
4
6
8
10
12
14
16
0
5
10
15
20
25
30
0
0.1
0.2
0.3
0.4
0.5
0.6

Fig. 1

Fig. 2

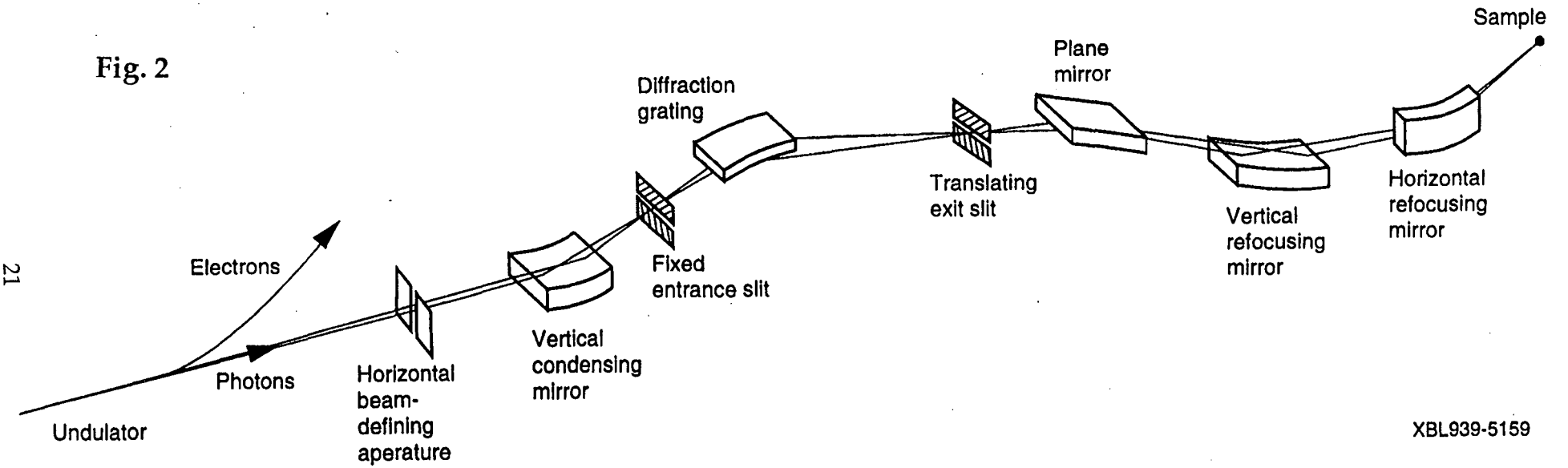
Sample
Plane mirror
Diffraction grating
Translating exit slit
Horizontal refocusing mirror
Vertical refocusing mirror
Fixed entrance slit
Electrons
Vertical condensing mirror
Photons
Horizontal beam-defining aperature
Undulator
XBL939-5159

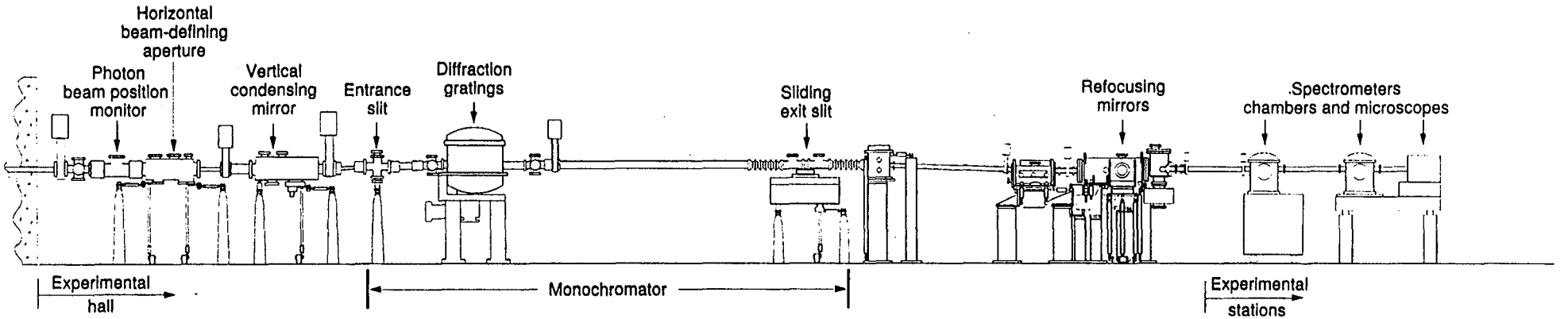
Horizontal beam-defining aperture
Photon beam position monitor
Vertical condensing mirror
Entrance slit
Diffraction gratings
Sliding exit slit
Refocusing mirrors
Spectrometers chambers and microscopes
Experimental hall
Monochromator
Experimental stations

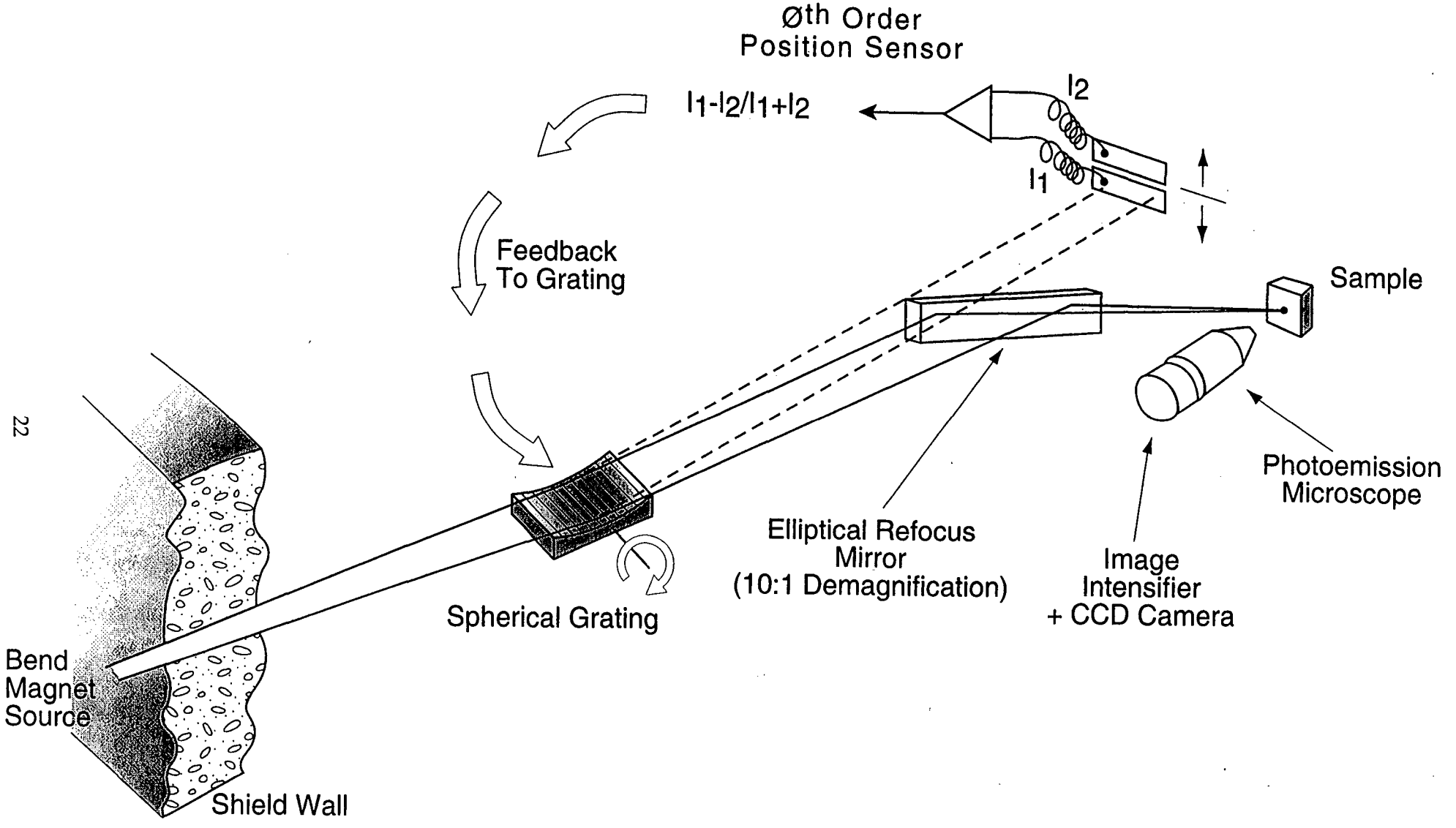
Øth Order
Position Sensor
I1-I2/I1+I2
I2
I1
Feedback
To Grating
Sample
Photoemission
Microscope
Elliptical Refocus
Mirror
(10:1 Demagnification)
Image
Intensifier
+ CCD Camera
Spherical Grating
Bend
Magnet
Source
Shield Wall

Fig. 3

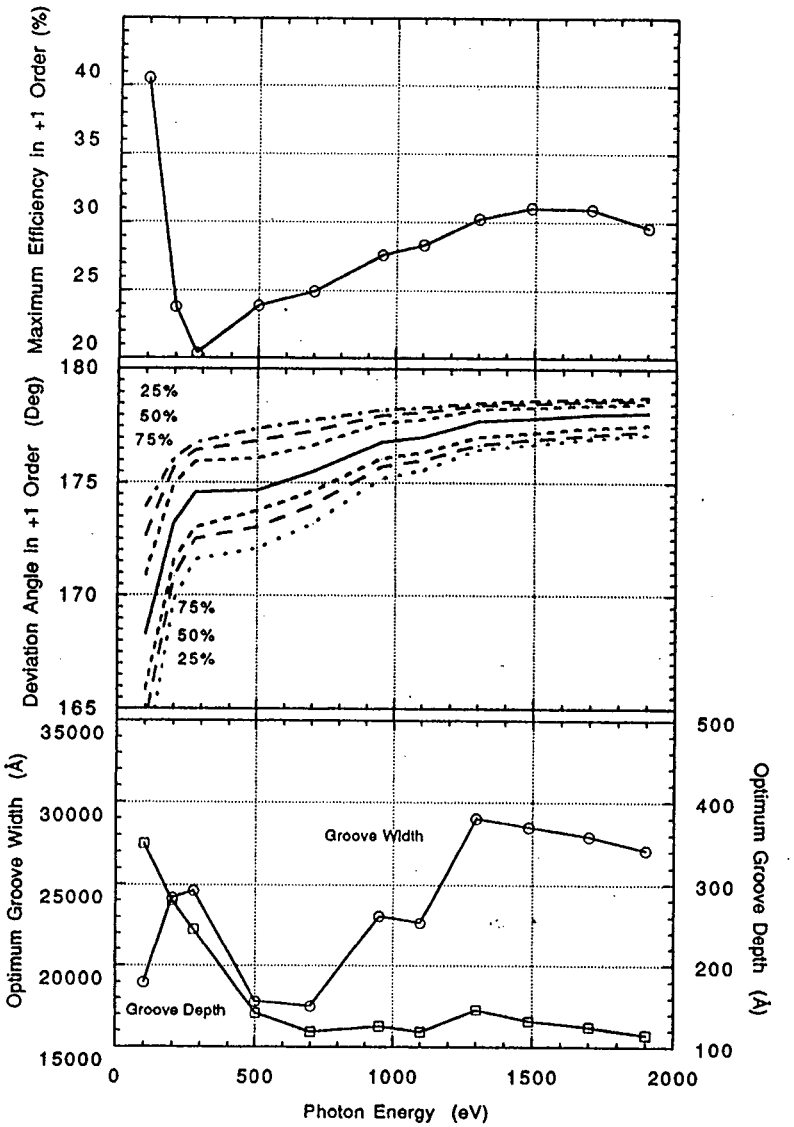
Maximum Efficiency in +1 Order (%)
Deviation Angle in +1 Order (Deg)
25%
50%
75%
75%
50%
25%
Optimum Groove Width (Å)
Groove Width
Groove Depth
Optimum Groove Depth (Å)
Photon Energy (eV)

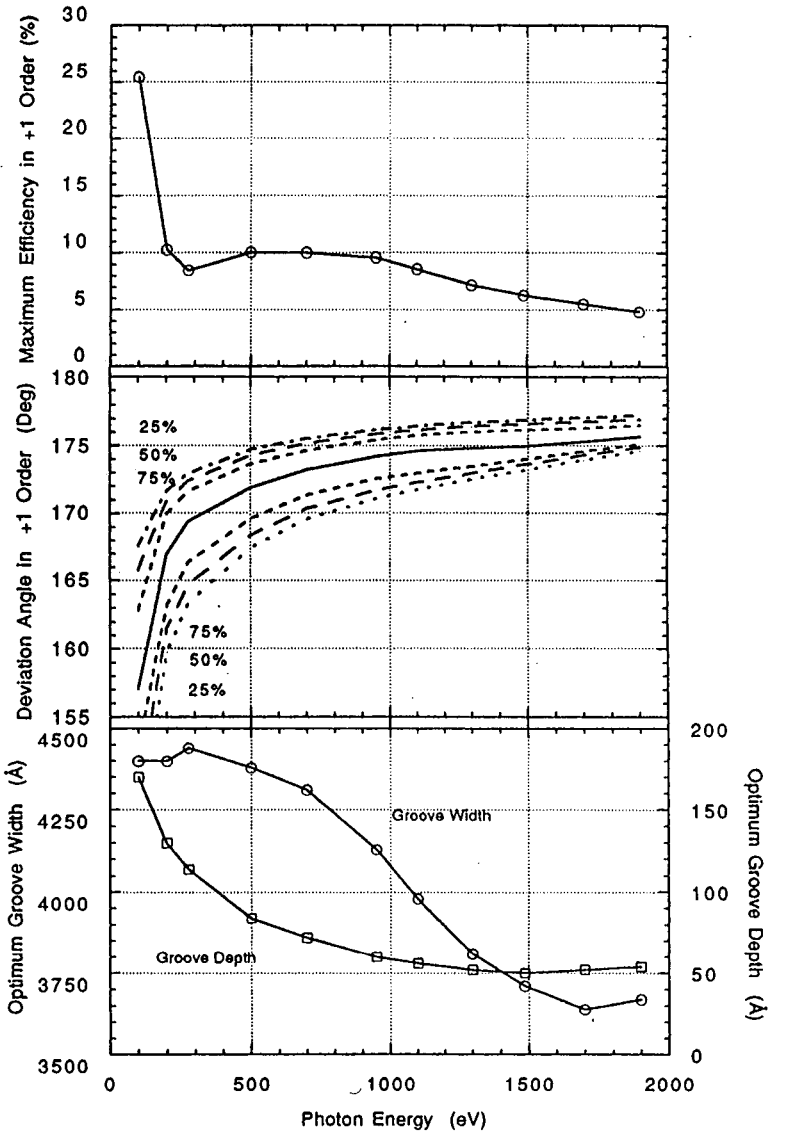
Maximum Efficiency in +1 Order (%)
Deviation Angle in +1 Order (Deg)
25%
50%
75%
75%
50%
25%
Optimum Groove Width (Å)
Groove Width
Groove Depth
Optimum Groove Depth (Å)
Photon Energy (eV)

Fig. 4

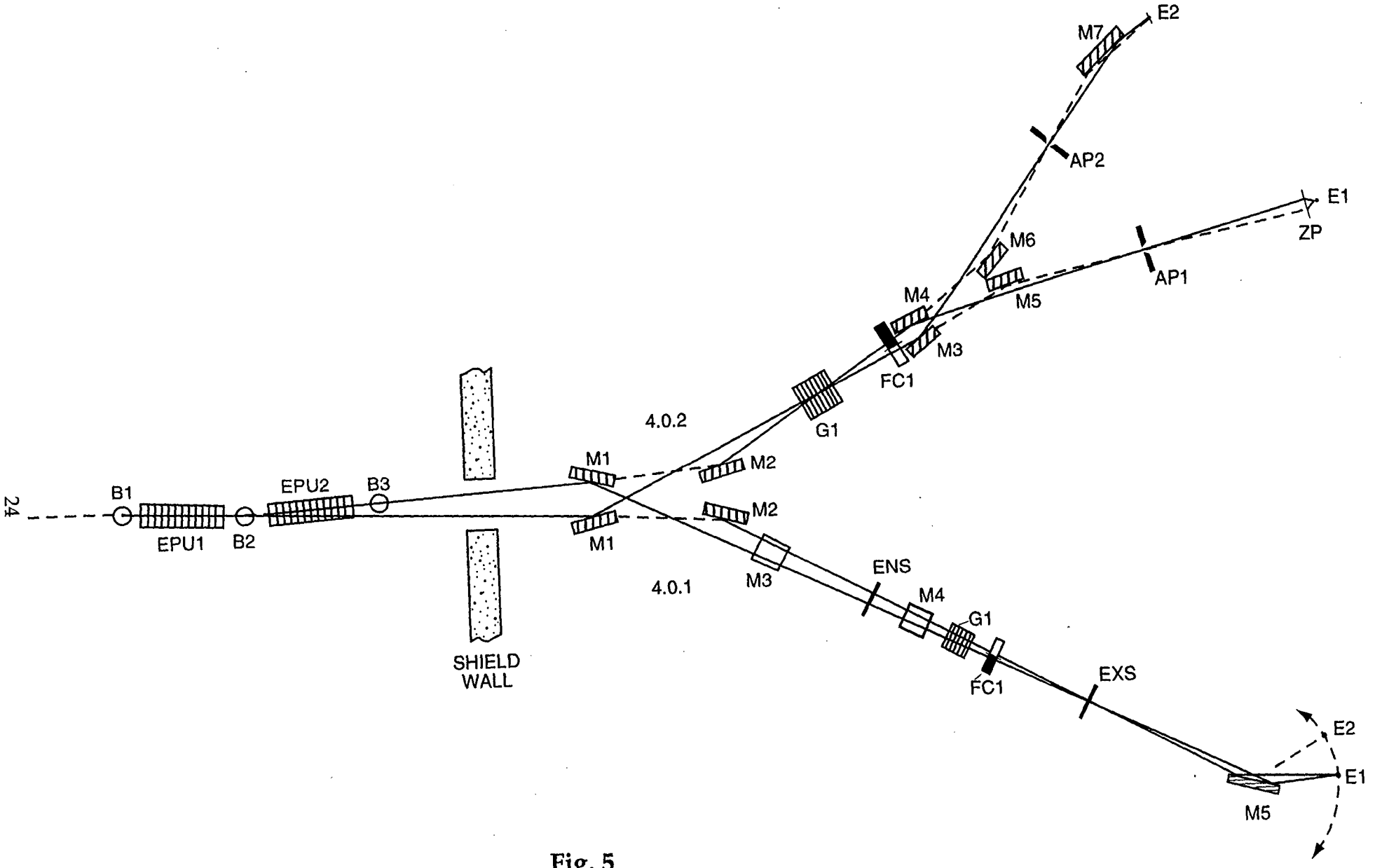
24
B1
EPU1
B2
EPU2
B3
SHIELD
WALL
M1
M2
M1
M2
4.0.2
4.0.1
G1
FC1
M3
M4
M5
M6
M7
AP2
AP1
E2
E1
ZP
M3
ENS
M4
G1
FC1
EXS
M5
E2
E1

Fig. 5

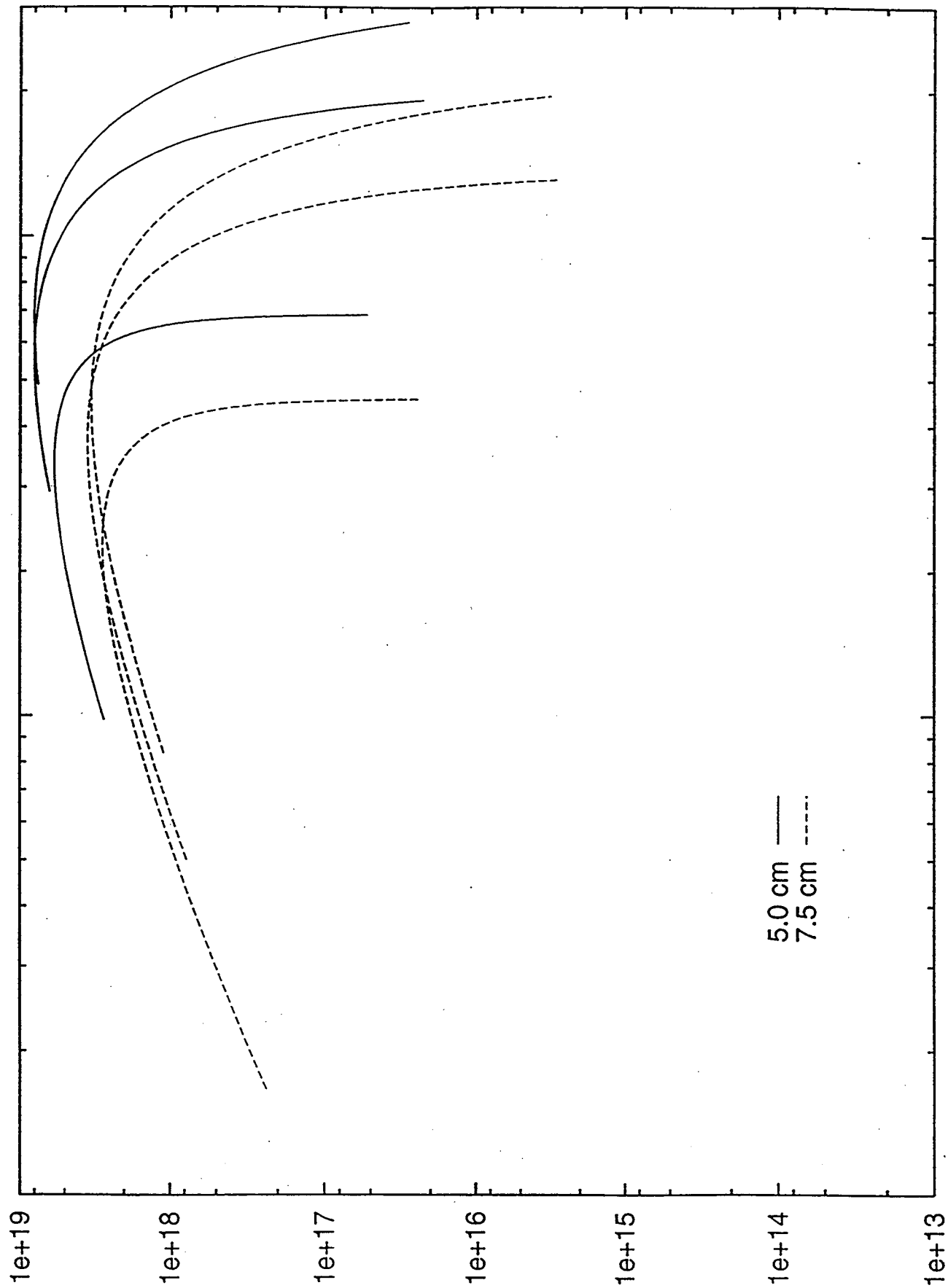
Merit Function Brightness
1e+19
1e+18
1e+17
1e+16
1e+15
1e+14
1e+13
10
100
1000
Photon Energy [eV]
5.0 cm
7.5 cm

Fig. 6

LAWRENCE BERKELEY LABORATORY
UNIVERSITY OF CALIFORNIA
TECHNICAL AND ELECTRONIC
INFORMATION DEPARTMENT
BERKELEY, CALIFORNIA 94720